Journal of Alloys and Compounds 709 (2017) 337–343

Contents lists available at ScienceDirect

Journal of Alloys and Compounds

journal homepage: http://www.elsevier.com/locate/jalcom

Deposition of CZTSe thin films and illumination effects on the device properties of Ag/n-Si/p-CZTSe/In heterostructure

Ö. Bayraklı [a, b, c, *], M. Terlemezoglu [a, b, d], H.H. Güllü [b, e], M. Parlak [a, b]

[a] Department of Physics, Middle East Technical University (METU), 06800, Ankara, Turkey
[b] Center for Solar Energy Research and Applications (GÜNAM), METU, 06800, Ankara, Turkey
[c] Department of Physics, Ahi Evran University, 40200, Kırşehir, Turkey
[d] Department of Physics, Namik Kemal University, 59030, Tekirdag, Turkey
[e] Central Laboratory, Middle East Technical University (METU), 06800, Ankara, Turkey

ARTICLE INFO

Article history:
Received 13 February 2017
Received in revised form
13 March 2017
Accepted 15 March 2017
Available online 16 March 2017

Keywords:
Thin film
Thermal evaporation
Kesterite
Heterostructure
Transmission

ABSTRACT

Characterization of $Cu_2ZnSnSe_4$ (CZTSe) thin films deposited by thermal evaporation sequentially from the pure elemental sources and in-situ post annealing was carried out at 400 C under Se evaporation atmosphere. Another annealing process was applied in nitrogen atmosphere at 450 °C to get poly-crystalline monophase CZTSe film structure. XRD analysis together with Raman spectroscopy was used to determine the structural properties. Spectral optical absorption coefficient evaluated from transmission data showed the band gap value of 1.49 eV for annealed film. Electrical measurements indicated that CZTSe thin films have p-type semiconductor behavior with the carrier density and mobility values of 10^{-19} cm^{-3} and 0.70 $cm^2/(V.s)$. Illumination effects on the device properties of Ag/n-Si/p-CZTSe/In heterostructure were investigated by analyzing current-voltage(I-V) and frequency dependent capacitance-voltage(C-V) data. Under the illumination, Ag/n-Si/p-CZTSe/In heterostructure showed photodiode behavior having V_{oc} value of 100 mV and I_{sc} value of 27.5 μA. With the illumination, series resistances (R_s), diode ideality factor (n) and barrier height (Φ_b) decreased and shunt resistance (R_{sh}) increased. Capacitance value at lower frequency decreased due to the illumination effect.

1. Introduction

Developments and research on thin film solar cells, such as CdTe and CIGS have still attraction due to their high power conversion efficiency over 22.1 and 22.3% respectively [1,2]. Nevertheless, in commercialization stage of these solar cells has some limitations owing to the toxicity, the shortage and the cost of Cd, In and Ga elements [3–5]. These restrictions have guided the works to search alternative materials of quaternary Cu_2-II-IV-VI_4 compounds [6,7]. Recently, several studies were reported on the family of compounds including $Cu_2ZnSnSe_4$ (CZTSe) and Cu_2ZnSnS_4(CZTS) structures as alternative for the popular film layers with theoretical efficiency value of 30% [8]. With similar physical properties to CIGS compounds, they become one of the most attractive absorber layers for the photovoltaic applications due to the abundance of Zn and Sn elements, low costs, non-toxicity, high absorption coefficient and suitable band gap [9]. In literature, kesterite thin films could be fabricated by various methods, including vacuum-based evaporations; thermal evaporation and magnetron sputtering deposition, non-vacuum based techniques such as; spin coating, electrodeposition and spray pyrolysis [10–25]. Through them, kesterite based thin film solar cell with the highest efficiency value of 12.6% was achieved by utilizing the hydrazine-based precursors technique [10]. Considering the highly toxic and explosive nature of hydrazine, this method is not suitable for the mass production. Due to the advantages on easily controlling the composition and crystalline structure in thin film fabrication and reproducibility for large scale production, vacuum based deposition methods are the most widely used techniques [26].

In device applications, the use of heterostructures is a considerable research field for determining and manipulating the electronic and optoelectronic properties of semiconductor devices [27]. Under these circumstances, constructing Si-based diode structure has been commonly point of interest in order to find the fundamental of diode characteristics of the synthesized thin film layer

* Corresponding author. Department of Physics, Middle East Technical University (METU), 06800, Ankara, Turkey. Tel.: +90 312 2107646; fax: +90 312 2105099.
E-mail address: ozgebayrakli@gmail.com (Ö. Bayraklı).

http://dx.doi.org/10.1016/j.jallcom.2017.03.163
0925-8388/

[28]. In electronic research field, Si-wafer is a popular material of choice due to well-known and established material with abundant and non-toxic characteristic [29,30,31].

In order to determine the structural, morphological and device behavior of CZTSe thin films, the deposition was carried out by sequentially onto soda-lime glass and n-Si wafer substrates from elemental sources by thermal evaporation. The investigation of the material properties of the obtained thin film structure was completed with X-ray Diffraction (XRD), Raman, Scanning Electron Microscopy (SEM) and Energy Dispersive X-ray Spectroscopy (EDS), optical transmission and Hall Effect measurements. Post-annealing process at 450 °C under N_2 atmosphere was applied to get the desired film properties. CZTSe thin films also deposited onto n-Si substrate to analyze the device characteristics of p-CZTSe/n-Si heterojunction. Current-Voltage (I-V) and capacitance-voltage (C-V) measurements were performed under dark and illuminated conditions. Then, the illumination effects on the device behavior of p-CZTSe/n-Si heterojunction were investigated. The results of the fabricated heterostructure give rectifying behavior and photovoltaic response to illumination. By combining polycrystalline CZTSe film layer with low cost Si wafer substrate, well-matched photovoltaic diode can be achieved [9]. The device performance indicates that CZTSe synthesized by thermal evaporation technique can be used as the absorber layer of solar cells.

2. Experimental details

CZTSe thin films were deposited by thermal evaporation method onto well cleaned soda lime glasses and one side polished 600 μm thick n-type Si with (100) orientation in a stacked layer formation. Deposition was carried out sequentially from 4N pure elemental (Cu,Sn.Zn,Se(Alfa Aesar, USA)) evaporation sources and during the deposition, substrate temperature was kept at room temperature and the vacuum was controlled at about 10^{-6} Torr. Following to the deposition of the stacked layers, the substrate temperature in-situ was increased slowly to 400 °C. The films were annealed at this temperature for an hour under Se evaporation (as grown). The thickness of the films was close to 700 nm after the deposition and selenization process. Furthermore, annealing process was applied under nitrogen atmosphere at 450 °C (annealed) to get the secondary and elemental phases free structural properties.

The structural properties of as-grown and annealed films were studied by XRD and Raman scattering spectroscopy measurements. In this study, X-ray measurements were performed by using a Rigaku Miniflex XRD system equipped with Cu Kα radiation source and Raman scattering experiments were performed by using Horiba Jobin Yvon Ihr550 imaging spectrometer including three grating monochromator. The thicknesses of the samples were measured by using Dektak 6M profilometer. The surface morphology and composition of the samples were studied by scanning electron microscope (SEM) equipped with energy dispersive X-ray analysis (EDAX) detector facility. Transmission spectra of the films were measured by using the Lambda 45 UV/VIS/NIR Spectrophotometer in the wavelength range of 300–900 nm to define the optical properties of CZTSe thin films. Room temperature resistivity and Hall Effect measurements were carried out at 0.9 Tesla using Nanomagnetic Hall Effect system.

In order to study the device behavior of Ag/n-Si/p-CZTSe/In heterojunction structure, Ag back ohmic contact annealed at 450 C before the evaporation of p-CZTSe films was deposited and following to the polished surface cleaning of n-Si wafer, Indium(In) dot ohmic contacts in 1 mm diameter using copper masks were coated by thermal metallic evaporation after thin film growth. To deduce the device characteristics of the fabricated Ag/n-Si/p-CZTSe/In heterojunction structure, it was analyzed by using current–voltage (I-V) and the room temperature capacitance-voltage (C-V) measurements for frequencies of 10 kHz and 1000 kHz under dark and illumination conditions. During these analyses, the computer-controlled measurement setup with a 2401 source measure unit, the Model 22 CTI Cryogenics closed-cycle helium cryostat and DRC-91C temperature controller were used. By the same way, the frequency dependent C-V measurements were carried out by using HP 4192A LF Impedance Analyzer.

3. Results and discussion

3.1. Characterization of CZTSe thin films

Atomic compositions of the deposited CZTSe thin films were given in Table 1, which was acquired from EDS measurement with ±2% uncertainty. When the results were analyzed, it showed that there are slight differences in the atomic composition of as-grown and annealed films after annealing process and both films are Zn-rich and Cu-deficient compositions. This is acceptable condition since Zn-rich composition may lead to improve the p-type conductivity and optical properties of deposited films [32,33].

As shown the XRD spectra of as-grown sample in Fig. 1, it has a polycrystalline CZTSe structure. However, the dominant peak observed in the spectra at $2\theta = 29.3^\circ$ and the other peak at $2\theta = 31.1^\circ$ may not be the characteristic phases of the CZTSe structure, since these phases match closely with ZnSe and CuSe diffraction peaks [11]. Further analysis must be done using Raman spectroscopy to be sure about the phases in the CZTSe structure. On the other hand, the XRD pattern of the sample subjected to annealing process showed that main diffraction peaks at $2\theta = 27.3^\circ$, 45.3° and 53.7° labeled as (112), (204) and (312) planes are the phases of CZTSe structure, and any secondary phases in the diffraction pattern with respect to (ICDD data #00-052-0868 CZTSe) weren't detected. Other reflections having low-intensity corresponding to CZTSe structure was also indexed in Fig. 1. The strongest peak of annealed sample at $2\theta = 27.3^\circ$ indexed as (112) plane was fitted using mixed of Gaussian and Lorentzian functions and full width at half maximum (FWHM) was found to be 0.229°. Then, using Scherrer's formula, crystallite size was approximated as 35.8 nm [12].

In addition to XRD analysis, Raman spectroscopy measurements were also applied further to investigate the secondary phases, but it is known that Raman spectroscopy is sensitive to the surface region instead of bulk region. In order to obtain the information about the phases related with the bulk and surface region, the grazing instance XRD measurements must be taken together with Raman analysis [34]. The Raman spectra of as-grown and annealed samples were given in Fig. 2. For an as-grown sample, it is shown that there are two peaks centered at 186 and 260 cm^{-1} which are attributed to $SnSe_2$ and CuSe, respectively [26,27,35,36]. This could be the indication of the secondary phase formation during the growth process but it isn't easy to resolve them in as grown form.

Table 1
EDS results for asgrown and annealed CZTSe thin films.

Sample	Chemical Compositions (at %)				Ratio of Compositions		
	Cu	Zn	Sn	Se	Cu/(Zn+Sn)	Zn/Sn	Se/(Cu+Zn+Sn)
As-grown	10	28	10	52	0.26	2.80	1.08
Annealed	10	31	9	50	0.25	3.44	1.00

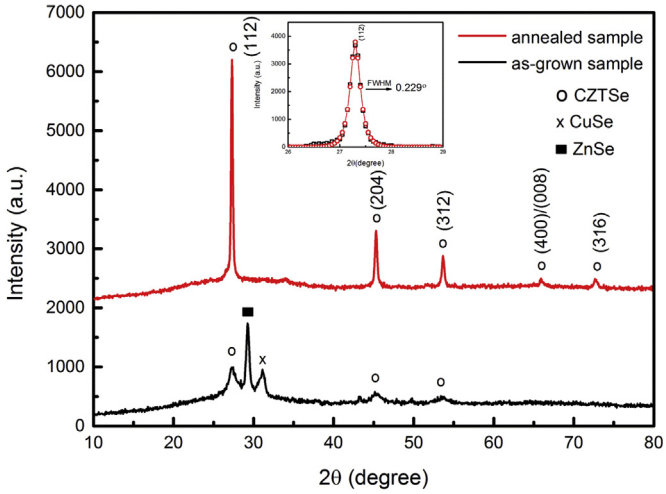

Fig. 1. XRD patterns for asgrown and annealed CZTSe thin films.

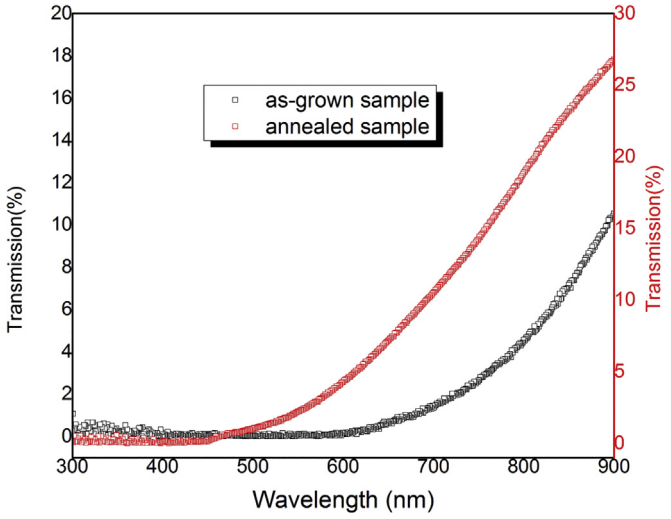

Fig. 3. Transmission spectra of asgrown and annealed CZTSe thin films.

On the other hand, observed peaks at 173, 196 and 233 cm^{-1} in Raman spectra of annealed film are the phases of CZTSe compound [32,37].

Transmission spectra in the wavelength range of 300–900 nm for asgrown and annealed CZTSe thin films were given in Fig. 3. The absorption coefficient and band gap value for the films were determined by using Tauc method and corresponding $(\alpha h\nu)^2$ vs hν plots are given in Fig. 4 [29,38]. The absorption coefficient was evaluated around 10^4 cm^{-1} and the band gap value was determined as 1.48 eV for both asgrown and annealed samples. Thus, the obtained result is consistent with the reported values in literature [39–42].

By the way, the room temperature electrical measurements indicated that CZTSe thin films have p-type semiconductor behavior and the resistivity value was obtained around 10^{-3} Ω cm. As a result of Hall effect measurement, the hole carrier density was calculated in the order of 10^{19} cm^{-3} and the mobility was obtained around 0.70 cm^2/V.s for CZTSe thin films.

3.2. Device properties of Ag/n-Si/p-CZTSe/In sandwich structure

The schematic diagram and cross sectional SEM micrographs for Ag/n-Si/p-CZTSe/In heterostructure were given in Fig. 5.

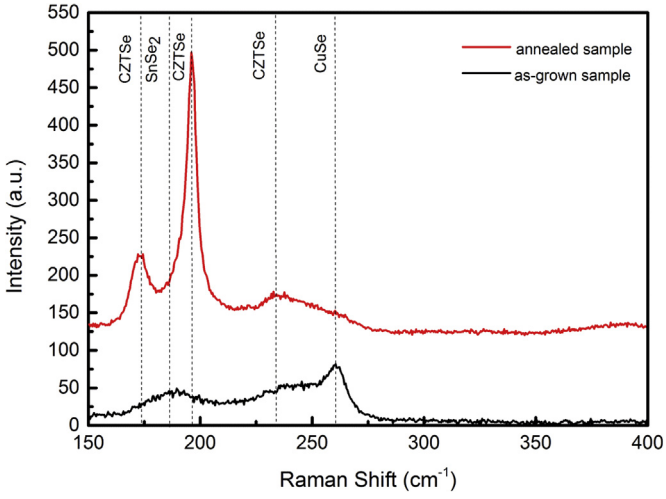

Fig. 2. Raman spectra for asgrown and annealed CZTSe thin films.

As seen from figure, SEM micrograph of the annealed film shows uniform surface morphology with thickness of ~670 nm that is almost the same average value measured by Dektak profilometer.

I-V characteristics for Ag/n-Si/p-CZTSe/In heterostructure were measured under dark and illuminated conditions at room temperature as given in Fig. 6. The behavior was analyzed by using standard diode expression;

$$I = I_0 \left[\exp\left(\frac{q(V - IR_s)}{nkT}\right) - 1\right] \quad (1)$$

where, I_0 is the reverse saturation current, V is the bias voltage, R_s is the series resistance, n is the ideality factor and k is the Boltzmann constant [15].

The reverse saturation current is given by the following relation;

$$I_0 = AA^*T^2 exp\left(-\frac{q\Phi_b}{kT}\right) \quad (2)$$

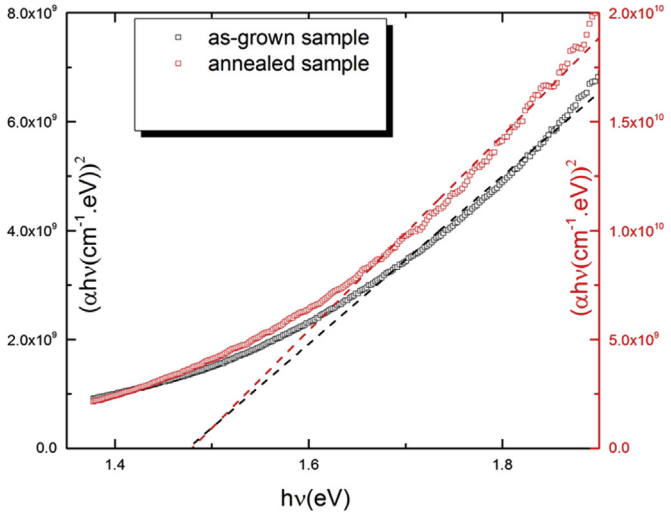

Fig. 4. $(\alpha h\nu)^2$ vs. hν plots of asgrown, and annealed CZTSe thin films.

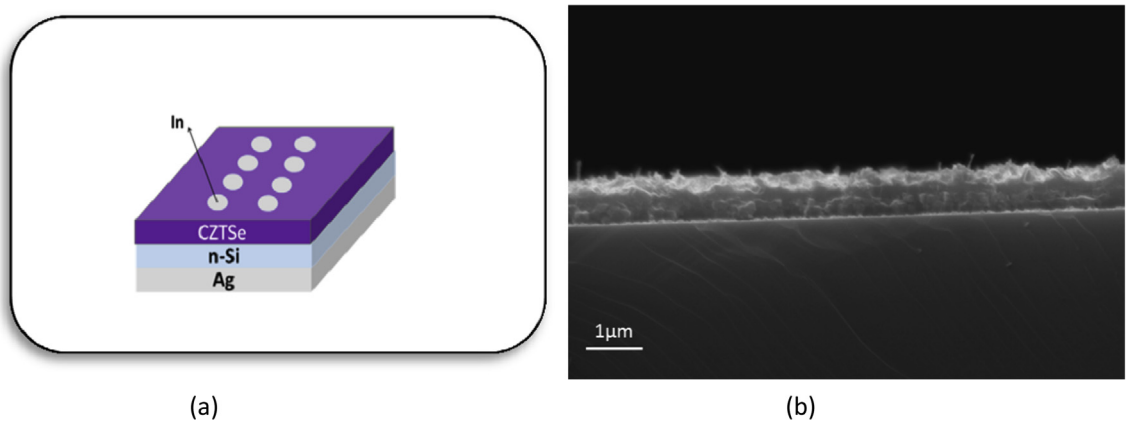

Fig. 5. (a) The schematic diagram of Ag/n-Si/p-CZTSe/In heterostructure and (b) cross sectional SEM micrograph of CZTSe film on glass substrate.

In this equation, ϕ_b is the potential barrier, A is the device area, A^* is Richardson constant for n-type Si, [43]. By using Eq. (1), the diode ideality factor "n" can be deduced as;

$$\frac{1}{n} = \frac{kT}{q}\frac{d(\ln(I))}{dV} \tag{3}$$

For the ideal contact, value of n should be equal to one where the pure thermionic emission mechanism is the dominant transport mechanism. However, for this structure it is greater than one, the contribution of the other transport mechanisms such as tunneling and recombination should be taken into account [10,44,45].

Fig. 6 points out ln(I) vs V plot for the heterostructure. By using this plot, experimental ϕ_b and n values were calculated from the current axis intercept and the slope of the linear region of the forward-bias region for both dark and illuminated conditions. While the barrier height ϕ_b and n values were calculated as 0.84 eV and 2.69 for the dark condition, 0.53 eV and 2.40 for illuminated condition, respectively According to the studies given in the literature on the similar Si-based heterostructure, the calculated room temperature n values are consistent with the reported values [6,7,46]. When the complete diode structure was considered, they were different from each other depending on Se and/or S contribution in the film structure and the calculated ϕ_b values were greater than the reported values [7,46]. On the other hand, Fig. 6 shows that the reverse current of the heterostructure increases with illumination. This increase was consistent with the generated carriers due to the light absorption and their contribution to the photocurrent [16].

As seen from I-V characteristics, they deviate from linearity both in forward and reverse bias voltages for each condition. At the high forward bias values, the junction resistance reaches to a constant value, which equals to R_s value. The same behavior occurs also in the reverse bias voltages leading to the determination R_{sh} value. The series resistance R_s is the resistance of the bulks and metallic contacts, on the other hand, the shunt resistance R_{sh} is responsible for the loss of the current at the edge of the device and the surface inhomogeneity [47,48]. R_s and R_{sh} are the parasitic resistances of the device structure and they were calculated by using the expression, $R_i = dV/dI$ [6,10,35,49].

In general, R_s in the diode has pronounced effect on the fill factor, and it could be the reason of low short-circuits current values. On the contrary, low R_{sh} value in the diode can provide an alternative conduction path for the light-generated current and therefore, it can pave the way for power losses in diodes. For dark and illuminated conditions, R_s values were obtained as 610 Ω and 379 Ω respectively. This reduction in the value of R_s with the illumination could also be the determination of the increase in the

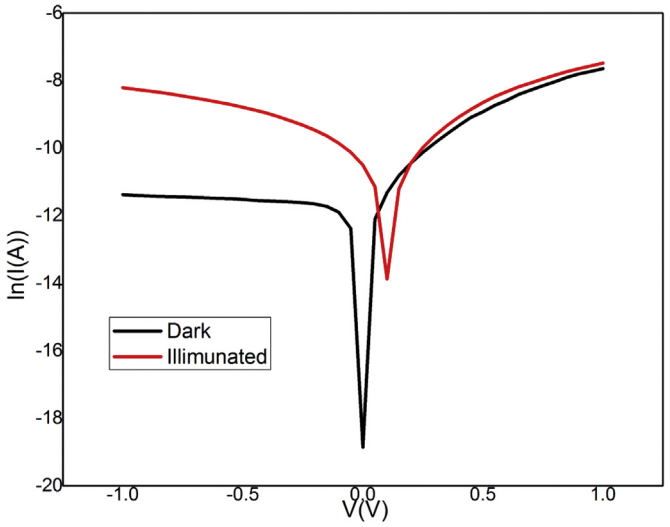

Fig. 6. ln(I) vs. V graph for Ag/n-Si/p-CZTSe/In heterostructure under dark and illuminated condition.

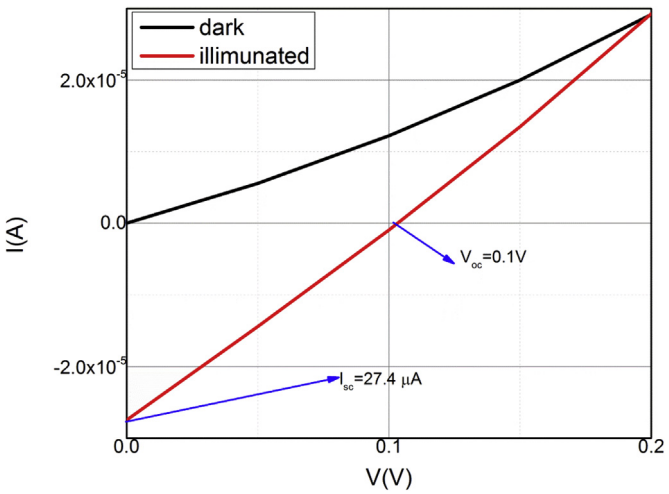

Fig. 7. I-V plot in the voltage range of 0–0.2 V for dark and illuminated condition.

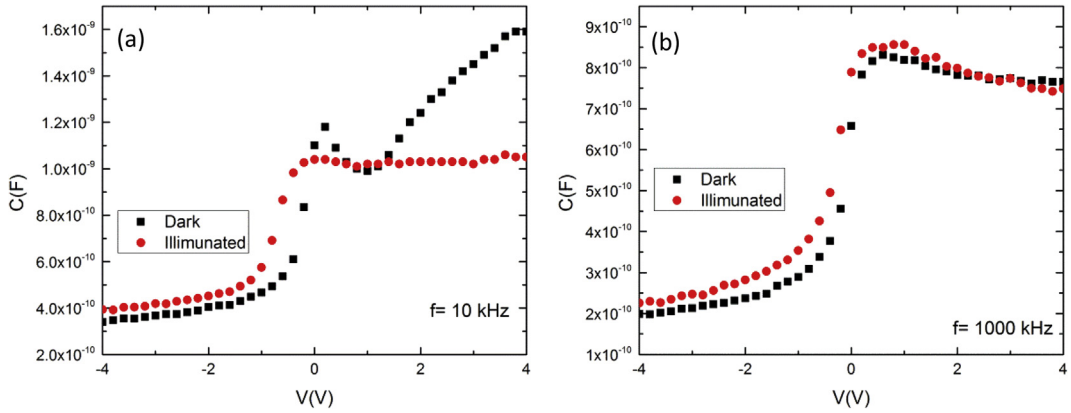

Fig. 8. Capacitance-Voltage (C-V) plots for the frequency of (a) 10 kHz (b) 1000 kHz under dark and illuminated conditions.

conductivity with the generated photocurrents [18]. Furthermore, R_{sh} values for the dark and the illuminated conditions were obtained as 2.8 MΩ and 3.8 MΩ respectively. The augmentation of the R_{sh} values with the illumination may be the indication of local inhomogeneities. They could lead to non- uniform flow of current across the heterojunction [50,51]. Shunt resistance is generally related with the localized defect regions and these regions become electrically active with the traps having larger concentrations. In fact, these traps could behave as cavity for majority carriers or light-generated minority carriers and they capture carriers from neighborhood regions [50,52]. When the heterojunction is illuminated with the light source, the trap starts getting filled and this reduces the shunt current that leads to increase in the shunt resistance of the diode [53,54].

Fig. 7 shows I-V plot in the voltage range of 0 and 0.2 V for both dark and illuminated conditions. These plots indicate that, Ag/n-Si/p-CZTSe/In heterostructure responses to illumination having the open circuit voltage (V_{oc}) value of 100 mV and the short circuit current I_{sc} value of 27.4 μA. Therefore, these values can be taken as the primary works in this fabrication of simple p-n junctions of kesterite thin films by n-Si substrate [9,27]. When the solar cell parameters obtained in this work were compared with the other studies, this device structure exhibits a good electronic behavior under solar illumination.

C-V measurements give information about built-in potential, carrier concentration, series resistance, surface states, etc. of the heterostructure. In order to get the information about these values, C-V measurements were carried out under both dark and illuminated conditions. And these measurements were done for different frequencies of 10 kHz and 1000 kHz for both conditions. Fig. 8 indicates that, in the higher frequency case, there is not a significant effect of the illumination on the C-V characteristics. However, for lower frequency under dark condition; the plot has a peak due to the presence of inter-face states. By the illumination, these states disappearing. Moreover, capacitance values decreased with the illumination. When the sample is illuminated, some of the electrons generated due to the illumination could be trapped, or the illumination may result in the release of the trapped electrons. These trapping and releasing processes can be considered as charging and discharging respectively. Moreover, they are random processes in the n-Si with the illumination and they may occur at the same time. When the charging process is dominant, capacitance decreases [55,56]. Moreover, the anomalous peak at zero bias, in the dark condition case, disappeared with the illumination. This disappearance may be consisted with the thermal effect due to the illumination [57].

C–V characteristics were analyzed by using the following expression;

$$\frac{1}{C^2} = \frac{2}{qN_d\varepsilon_o\varepsilon_s A^2}(V_{bi} - V) \tag{4}$$

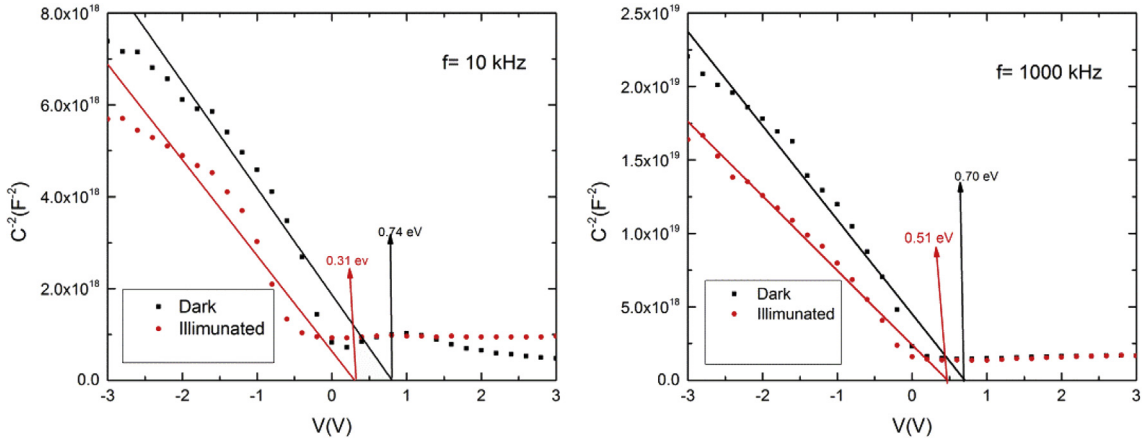

Fig. 9. C-2 vs V plot for the frequency of (a) 10 kHz and (b) 1000 kHz under dark and illuminated conditions.

Table 2
The calculated device parameters from the slope and intercept values of C^{-2} vs V plot.

Condition	V_{bi} (eV)	N_d (cm^{-3}) × 10^{16}	Φ(eV)
10 kHz (dark)	0.70	3.35	0.87
10 kHz (illuminated)	0.51	4.21	0.67
1000 kHz (dark)	0.74	9.29	0.88
1000 kHz (illuminated)	0.34	10.3	0.49

$$N_d = \frac{2}{q\varepsilon_O\varepsilon_S A^2\left[\frac{d}{dV}\left(\frac{1}{C^2}\right)\right]} \quad (5)$$

here V_{bi} is the built-in potential, N_d is the donor concentration. ε_o is the permittivity of free space, ε_s is the dielectric constant of Si (11.7) and A is the diode area.

C^{-2} vs V plots for different frequencies are shown in Fig. 9. Their variations are linear with the intercept on voltage axis which gives the built-in potential and from the slope of this plot; carrier concentration (N_d) can be calculated by using equation-5. Moreover, the barrier heights (Φ_b) of the heterojunction diode can be calculated from the equation;

$$\Phi_b = V_{bi} + \frac{kT}{q}\ln\left(\frac{N_C}{N_d}\right) \quad (6)$$

where N_c is the effective density of state in the conduction band ($N_c = 2.8 \times 10^{19} cm^{-3}$). All results for all conditions are tabulated in Table 2. As seen from Table 2, illumination led to increase in N_d values and decrease in V_{bi} and Φ_b values due to photo-generated carriers. Moreover, the barrier height values in dark condition obtained from I-V measurements were comparable with the values obtained from C-V analysis.

4. Conclusion

In this study; structural, optical and electrical characterization of CZTSe thin films and the device behavior of for Ag/n-Si/p-CZTSe/In heterostructure were analyzed. According to structural characterization, post-annealing process under N atmosphere at 450 °C must be applied to get the desired film properties. The band gap energy values were obtained as 1.45 and 1.49 eV for asgrown and annealed films, respectively. CZTSe films have p-type semiconductor behavior as observed from Hall voltage and hot probe measurements. I-V analysis of Ag/n-Si/p-CZTSe/In heterostructure showed that, Rs value reduced under illumination. This could be taken as the contribution of photo generated carriers for the increase in the conductivity. C-V analysis indicated that the heterojunction device parameters were completely related with the trap and interface states, so that the illumination may initiate the release of the trapped charges depending on the characteristics of trap levels and/or impurity states. This can be considered as the charging and discharging effect. Ag/n-Si/p-CZTSe/In heterostructure has a photodiode behavior having the V_{oc} value of 100 mV and I_{sc} value of 27.4 μA. This study can initiate the studies which aim to develop a tandem structure based on well- developed high efficiency CZTSe or CZTS solar cells in long term.

References

[1] X. Jin, C. Yuan, L. Zhang, G. Jiang, W. Liu, C. Zhu, Solar Energy Materials & Solar Cells Pulsed laser deposition of Cu 2 ZnSn (S x Se 1 Àx) 4 thin fi lm solar cells using quaternary oxide target prepared by combustion method, Sol. Energy Mater. Sol. Cells 155 (2016) 216–225, http://dx.doi.org/10.1016/j.solmat.2016.12.042.

[2] Y.-P. Lin, T.-E. Hsieh, Y.-C. Chen, K.-P. Huang, Characteristics of Cu2ZnSn(SxSe1−x)4 thin-film solar cells prepared by sputtering deposition using single quaternary Cu2ZnSnS4 target followed by selenization/sulfurization treatment, Sol. Energy Mater. Sol. Cells 162 (2017) 55–61, http://dx.doi.org/10.1016/j.solmat.2016.12.042.

[3] R. Pandiyan, Z. Oulad Elhmaidi, Z. Sekkat, M. Abd-lefdil, M.A. El Khakani, Reconstructing the energy band electronic structure of pulsed laser deposited CZTS thin films intended for solar cell absorber applications, Appl. Surf. Sci. 396 (2016) 1562–1570, http://dx.doi.org/10.1016/j.apsusc.2016.11.210.

[4] M.A. Green, Consolidation of thin-film photovoltaic technology: the coming decade of opportunity, Prog. Photovolt. Res. Appl. 14 (2006) 383–392, http://dx.doi.org/10.1002/pip.702.

[5] J.J. Scragg, P.J. Dale, L.M. Peter, G. Zoppi, I. Forbes, New routes to sustainable photovoltaics: evaluation of Cu 2 ZnSnS 4 as an alternative absorber material, Phys. Status Solidi 245 (2008) 1772–1778, http://dx.doi.org/10.1002/pssb.200879539.

[6] H. Matsushita, T. Maeda, A. Katsui, T. Takizawa, Thermal analysis and synthesis from the melts of Cu-based quaternary compounds Cu–III–IV–VI4 and Cu2–II–IV–VI4 (II=Zn,Cd; III=Ga,In; IV=Ge,Sn; VI=Se), J. Cryst. Growth 208 (2000) 416–422, http://dx.doi.org/10.1016/S0022-0248(99)00468-6.

[7] I.D. Olekseyuk, L.D. Gulay, I.V. Dydchak, L.V. Piskach, O.V. Parasyuk, O.V. Marchuk, Single crystal preparation and crystal structure of the Cu2Zn/Cd,Hg/SnSe4 compounds, J. Alloys Compd. 340 (2002) 141–145, http://dx.doi.org/10.1016/S0925-8388(02)00006-3.

[8] W. Shockley, H.J. Queisser, Detailed balance limit of efficiency of pn junction solar cells detailed balance limit of efficiency of p-n junction solar cells*, J. Appl. Phys. Addit. Inf. J. Appl. Phys. J. Homepage 32 (1961), http://dx.doi.org/10.1063/1.1736034.

[9] N. Song, M. Young, F. Liu, P. Erslev, S. Wilson, S.P. Harvey, G. Teeter, Y. Huang, X. Hao, M.A. Green, Epitaxial Cu2ZnSnS4 thin film on Si (111) 4° substrate, Appl. Phys. Lett. 106 (2015) 252102, http://dx.doi.org/10.1063/1.4922992.

[10] K. Tanaka, M. Oonuki, N. Moritake, H. Uchiki, Cu2ZnSnS4Cu2ZnSnS4 thin film solar cells prepared by non-vacuum processing, Sol. Energy Mater. Sol. Cells 93 (2009) 583–587, http://dx.doi.org/10.1016/j.solmat.2008.12.009.

[11] Y.-P. Lin, Y.-F. Chi, T.-E. Hsieh, Y.-C. Chen, K.-P. Huang, Preparation of Cu2ZnSnS4 (CZTS) sputtering target and its application to the fabrication of CZTS thin-film solar cells, J. Alloys Compd. 654 (2016) 498–508, http://dx.doi.org/10.1016/j.jallcom.2015.09.111.

[12] A. Nagaoka, K. Yoshino, H. Taniguchi, T. Taniyama, H. Miyake, Preparation of Cu2ZnSnS4 single crystals from Sn solutions, J. Cryst. Growth 341 (2012) 38–41, http://dx.doi.org/10.1016/j.jcrysgro.2011.12.046.

[13] H. Katagiri, Cu2ZnSnS4 thin film solar cells, Thin Solid Films 480–481 (2005) 426–432, http://dx.doi.org/10.1016/j.tsf.2004.11.024.

[14] H. Katagiri, K. Saitoh, T. Washio, H. Shinohara, T. Kurumadani, S. Miyajima, Development of thin film solar cell based on Cu2ZnSnS4 thin films, Sol. Energy Mater. Sol. Cells 65 (2001) 141–148, http://dx.doi.org/10.1016/S0927-0248(00)00088-X.

[15] B. Shin, O. Gunawan, Y. Zhu, N.A. Bojarczuk, S.J. Chey, S. Guha, Thin film solar cell with 8.4% power conversion efficiency using an earth-abundant Cu 2 ZnSnS 4 absorber, Prog. Photovolt. Res. Appl. 21 (2013) 72–76, http://dx.doi.org/10.1002/pip.1174.

[16] S.M. Lee, Y.S. Cho, Characteristics of Cu2ZnSnSe4 and Cu2ZnSn(Se,S)4 absorber thin films prepared by post selenization and sequential sulfurization of co-evaporated Cu–Zn–Sn precursors, J. Alloys Compd. 579 (2013) 279–283, http://dx.doi.org/10.1016/j.jallcom.2013.06.064.

[17] X. Jiang, L. Shao, J. Zhang, J. Chen, Preparation and characterization of Cu2ZnSn(S x Se1−x)4 thin films by synchronous sulfo-selenization of single-source evaporated metallic precursors, Acta Metall. Sin. Engl. Lett. 27 (2014) 689–693, http://dx.doi.org/10.1007/s40195-014-0098-3.

[18] L. Grenet, S. Bernardi, D. Kohen, C. Lepoittevin, S. Noël, N. Karst, A. Brioude, S. Perraud, H. Mariette, Cu2ZnSn(S1−xSex)4 based solar cell produced by selenization of vacuum deposited precursors, Sol. Energy Mater. Sol. Cells 101 (2012) 11–14, http://dx.doi.org/10.1016/j.solmat.2012.02.016.

[19] J. Li, H. Wang, M. Luo, J. Tang, C. Chen, W. Liu, F. Liu, Y. Sun, J. Han, Y. Zhang, 10% Efficiency Cu2ZnSn(S,Se)4 thin film solar cells fabricated by magnetron sputtering with enlarged depletion region width, Sol. Energy Mater. Sol. Cells 149 (2016) 242–249, http://dx.doi.org/10.1016/j.solmat.2016.02.002.

[20] X. Lv, Q. Liu, C. Zhu, Z. Wang, Characterization of Cu2ZnSn(S,Se)4 film by selenizing Cu2ZnSnS4 precursor film from co-sputtering process, Mater. Lett. 180 (2016) 68–71, http://dx.doi.org/10.1016/j.matlet.2016.04.039.

[21] B.-T. Jheng, K.-M. Huang, S.-F. Chen, M.-C. Wu, Effects of substrate temperature on the Cu2ZnSnS4 films deposited by radio-frequency sputtering with single target, Thin Solid Films 564 (2014) 345–350, http://dx.doi.org/10.1016/j.tsf.2014.05.053.

[22] D.A.R. Barkhouse, O. Gunawan, T. Gokmen, T.K. Todorov, D.B. Mitzi, Device characteristics of a 10.1% hydrazine-processed Cu2ZnSn(Se,S)4 solar cell, Prog. Photovolt. Res. Appl. 20 (2012) 6–11, http://dx.doi.org/10.1002/pip.1160.

[23] P.K. Nayak, D. Cahen, Updated assessment of possibilities and limits for solar cells, Adv. Mater. 26 (2014) 1622–1628, http://dx.doi.org/10.1002/adma.201304620.

[24] T. Slimani Tlemcani, F.C. El Moursli, M. Taibi, F. Hajji, E.B. Benamar, S. Colis, G. Schmerber, D. Muller, A. Slaoui, A. Dinia, M. Abd-Lefdil, One step electrodeposited CZTS thin films: preparation and characterization, in: 2014 Int. Renew. Sustain. Energy Conf, IEEE, 2014, pp. 89–93, http://dx.doi.org/10.1109/IRSEC.2014.7059867.

[25] O. Vigil-Galán, M. Courel, M. Espindola-Rodriguez, D. Jiménez-Olarte, M. Aguilar-Frutis, E. Saucedo, Electrical properties of sprayed Cu2ZnSnS4 thin films and its relation with secondary phase formation and solar cell performance, Sol. Energy Mater. Sol. Cells 132 (2015) 557–562, http://dx.doi.org/10.1016/j.solmat.2014.10.009.
[26] H. Wang, Progress in thin film solar cells based on Cu 2 ZnSnS 4, Int. J. Photoenergy 2011 (2011) 1–10, http://dx.doi.org/10.1155/2011/801292.
[27] C.-H. Ruan, Y.-J. Lin, Y.-H. Chen, H.-C. Chang, Rectifying performance of p-type tin(II) sulfide contacts on n-type silicon: effect of silicon nanowire sulfidation on electronic transport of heterojunction diodes, Mater. Sci. Semicond. Process 32 (2015) 62–67, http://dx.doi.org/10.1016/j.mssp.2015.01.005.
[28] Y.-J. Lin, C.-H. Ruan, Y.-J. Chu, C.-J. Liu, F.-H. Lin, Correlation between interface modification and rectifying behavior of p-type Cu2ZnSnS4/n-type Si diodes, Appl. Phys. A 121 (2015) 103–108, http://dx.doi.org/10.1007/s00339-015-9390-y.
[29] R. Jansen, J.S. Moodera, Electrical and photoelectrical properties of Si/In–Te heterojunctions, Appl. Phys. Lett. (1999), http://dx.doi.org/10.1063/1.124929. http://oasc12039.247realmedia.com/RealMedia/ads/click_lx.ads/www.aip.org/pt/adcenter/pdfcover_test/L-37/281601297/x01/AIP-PT/APR_APLArticleDL_022217/APRconf_1640x440Banner_12-16B.jpg/434f71374e315a556e61414141774c75?x.
[30] F.A. Akgul, G. Akgul, H.H. Gullu, H.E. Unalan, R. Turan, Enhanced diode performance in cadmium telluride–silicon nanowire heterostructures, J. Alloys Compd. 644 (2015) 131–139, http://dx.doi.org/10.1016/j.jallcom.2015.04.195.
[31] C.-C. Huang, Y.-J. Lin, C.-J. Liu, Y.-W. Yang, Photovoltaic properties of n-type SnS contact on the unpolished p-type Si surfaces with and without sulfide treatment, Microelectron. Eng. 110 (2013) 21–24, http://dx.doi.org/10.1016/j.mee.2013.04.030.
[32] A. Fairbrother, X. Fontané, V. Izquierdo-Roca, M. Placidi, D. Sylla, M. Espindola-Rodriguez, S. López-Mariño, F.A. Pulgarín, O. Vigil-Galán, A. Pérez-Rodríguez, E. Saucedo, Secondary phase formation in Zn-rich Cu 2 ZnSnSe 4 -based solar cells annealed in low pressure and temperature conditions, Prog. Photovolt. Res. Appl. 22 (2014) 479–487, http://dx.doi.org/10.1002/pip.2473.
[33] G. Zoppi, I. Forbes, R.W. Miles, P.J. Dale, J.J. Scragg, L.M. Peter, Cu 2 ZnSnSe 4 thin film solar cells produced by selenisation of magnetron sputtered precursors, Prog. Photovolt. Res. Appl. 17 (2009) 315–319, http://dx.doi.org/10.1002/pip.886.
[34] P.M.P. Salom, P.A. Fernandes, J.P. Leit??o, M.G. Sousa, J.P. Teixeira, A.F. Da Cunha, Secondary crystalline phases identification in Cu2ZnSnSe 4thin films: contributions from Raman scattering and photoluminescence, J. Mater. Sci. 49 (2014) 7425–7436, http://dx.doi.org/10.1007/s10853-014-8446-2.
[35] A.V. Moholkar, S.S. Shinde, G.L. Agawane, S.H. Jo, K.Y. Rajpure, P.S. Patil, C.H. Bhosale, J.H. Kim, Studies of compositional dependent CZTS thin film solar cells by pulsed laser deposition technique: an attempt to improve the efficiency, J. Alloys Compd. 544 (2012) 145–151, http://dx.doi.org/10.1016/j.jallcom.2012.07.108.
[36] S. Ranjbar, M.R. Rajesh Menon, P.A. Fernandes, A.F. da Cunha, Effect of selenization conditions on the growth and properties of Cu2ZnSn(S,Se)4 thin films, Thin Solid Films 582 (2015) 188–192, http://dx.doi.org/10.1016/j.tsf.2014.11.044.
[37] D.H. Kuo, M. Tsega, The investigation of CuxZnSnSe4 bulks with x = 1.4-2.2 for debating the Cu excess and Cu deficiency used in thin-film solar cells, Mater. Res. Bull. 49 (2014) 608–613, http://dx.doi.org/10.1016/j.materresbull.2013.10.009.
[38] O.P. Singh, N. Vijayan, K.N. Sood, B.P. Singh, V.N. Singh, Controlled substitution of S by Se in reactively sputtered CZTSSe thin films for solar cells, J. Alloys Compd. 648 (2015) 595–600, http://dx.doi.org/10.1016/j.jallcom.2015.06.276.
[39] J. Henry, K. Mohanraj, G. Sivakumar, Electrical and optical properties of CZTS thin films prepared by SILAR method, J. Asian Ceram. Soc. 4 (2015) 81–84, http://dx.doi.org/10.1016/j.jascer.2015.12.003.
[40] S.K. Saha, A. Guchhait, A.J. Pal, Cu2ZnSnS4 (CZTS) nanoparticle based nontoxic and earth-abundant hybrid pn-junction solar cells, Phys. Chem. Chem. Phys. 14 (2012) 8090, http://dx.doi.org/10.1039/c2cp41062a.
[41] S. Ahn, S. Jung, J. Gwak, A. Cho, K. Shin, K. Yoon, D. Park, H. Cheong, J.H. Yun, Determination of band gap energy (Eg) of Cu2 ZnSnSe4 thin films: on the discrepancies of reported band gap values, Appl. Phys. Lett. 97 (2010) 2–4, http://dx.doi.org/10.1063/1.3457172.
[42] G. Suresh Babu, Y.B. Kishore Kumar, P. Uday Bhaskar, S. Raja Vanjari, Effect of Cu/(Zn+Sn) ratio on the properties of co-evaporated Cu2ZnSnSe4 thin films, Sol. Energy Mater. Sol. Cells 94 (2010) 221–226, http://dx.doi.org/10.1016/j.solmat.2009.09.005.
[43] S.M. Sze, K.K. Ng, Physics of Semiconductor Devices, third ed., Springer International Publishing, Cham, 2014 http://dx.doi.org/10.1007/978-3-319-03002-9.
[44] K. Jimbo, R. Kimura, T. Kamimura, S. Yamada, W.S. Maw, H. Araki, K. Oishi, H. Katagiri, Cu2ZnSnS4-type thin film solar cells using abundant materials, Thin Solid Films 515 (2007) 5997–5999, http://dx.doi.org/10.1016/j.tsf.2006.12.103.
[45] B.-A. Schubert, B. Marsen, S. Cinque, T. Unold, R. Klenk, S. Schorr, H.-W. Schock, Cu2ZnSnS4 thin film solar cells by fast coevaporation, Prog. Photovolt. Res. Appl. 19 (2011) 93–96, http://dx.doi.org/10.1002/pip.976.
[46] Y.J. Lin, C.H. Ruan, Y.J. Chu, C.J. Liu, F.H. Lin, Correlation between interface modification and rectifying behavior of p-type Cu_2ZnSnS_4/n-type Si diodes, Appl. Phys. A Mater. Sci. Process 121 (2015) 103–108, http://dx.doi.org/10.1007/s00339-015-9390-y.
[47] F. Yakuphanoglu, Nanostructure Cu2ZnSnS4 thin film prepared by sol–gel for optoelectronic applications, Sol. Energy 85 (2011) 2518–2523, http://dx.doi.org/10.1016/j.solener.2011.07.012.
[48] A. Ennaoui, M. Lux-Steiner, A. Weber, D. Abou-Ras, I. Kötschau, H.-W. Schock, R. Schurr, A. Hölzing, S. Jost, R. Hock, T. Voß, J. Schulze, A. Kirbs, Cu2ZnSnS4 thin film solar cells from electroplated precursors: novel low-cost perspective, Thin Solid Films 517 (2009) 2511–2514, http://dx.doi.org/10.1016/j.tsf.2008.11.061.
[49] J.Y. Kim, K. Lee, N.E. Coates, D. Moses, T.-Q. Nguyen, M. Dante, A.J. Heeger, Efficient tandem polymer solar cells fabricated by all-solution processing, Science (80-.) 317 (2007) 222–225, http://dx.doi.org/10.1126/science.1141711.
[50] F. Khan, S.N. Singh, M. Husain, Effect of illumination intensity on cell parameters of a silicon solar cell, Sol. Energy Mater. Sol. Cells 94 (2010) 1473–1476, http://dx.doi.org/10.1016/j.solmat.2010.03.018.
[51] B.C. Chakravarty, N.K. Arora, S.N. Singh, B.K. Das, Solar cell performance with an inhomogeneous grain size distribution, IEEE Trans. Electron Devices 33 (1986) 158–160, http://dx.doi.org/10.1109/T-ED.1986.22455.
[52] D.V. Lang, Deep-level transient spectroscopy: a new method to characterize traps in semiconductors, J. Appl. Phys. 45 (1974) 3023–3032, http://dx.doi.org/10.1063/1.1663719.
[53] S.N. Singh, D. Kumar, Phenomenological model of anomalously high photovoltages generated in obliquely deposited semiconductor films, J. Appl. Phys. 103 (2008) 23713, http://dx.doi.org/10.1063/1.2828009.
[54] E. Cuce, P.M. Cuce, T. Bali, An experimental analysis of illumination intensity and temperature dependency of photovoltaic cell parameters, Appl. Energy 111 (2013) 374–382, http://dx.doi.org/10.1016/j.apenergy.2013.05.025.
[55] K. Sumino, Defect Control in Semiconductors, Elsevier, 1990.
[56] M. Yang, T.P. Chen, L. Ding, Y. Liu, F.R. Zhu, S. Fung, Capacitance switching in SiO2 thin film embedded with Ge nanocrystals caused by ultraviolet illumination, Appl. Phys. Lett. 95 (2009), http://dx.doi.org/10.1063/1.3224191.
[57] S.A. Arzhannikova, M.D. Efremov, V.A. Volodin, G.N. Kamaev, D.V. Marin, V.S. Shevchuk, S.A. Kochubei, A.A. Popov, Y.A. Minakov, Photoinduced variation of capacitance characteristics of MDS structures with three-layer SiN_x dielectrics, Solid State Phenom. 131–133 (2008) 461–466, http://dx.doi.org/10.4028/www.scientific.net/SSP.131-133.461.